

Ab initio study of 2p-core level x-ray photoemission spectra in ferromagnetic transition metals

Manabu Takahashi¹ and Jun-ichi Igarashi²

¹*Faculty of Engineering, Gunma University, Kiryu, Gunma 376-8515, Japan*

²*Faculty of Science, Ibaraki University, Mito, Ibaraki 310-8512, Japan*

We study the 2p-core level x-ray photoemission spectra in ferromagnetic transition metals, Fe, Co, and Ni using a recently developed *ab initio* method. The excited final states are set up by distributing electrons on the one-electron states calculated under the fully screened potential in the presence of the core hole. We evaluate the overlap between these excited states and the ground state by using one-electron wave functions, and obtain the spectral curves as a function of binding energy. The calculated spectra reproduce well the observed spectra displaying interesting dependence on the element and on the spin of the removed core electron. The origin of the spectral shapes is elucidated in terms of the one-electron states screening the core hole. The magnetic splitting of the threshold energy is also estimated by using the coherent potential approximation within the fully screened potential approximation. It decreases more rapidly than the local spin moment with moving from Fe to Ni. It is estimated to be almost zero for Ni despite the definite local moment about $0.6 \mu_B$, in agreement with the experiment.

PACS numbers: 79.60.-i 71.15.Qe 71.20.Be

I. INTRODUCTION

Core-level x-ray photoemission spectroscopy (XPS) is one of the powerful tools for studying the electronic structure in solids through the response of electrons to the photogenerated core hole. It is well known that the response function in metals displays singular behavior near the Fermi edge.¹⁻³ Core-level XPS spectra as a function of binding energy display asymmetric shape near the threshold.⁴ The spectra sometimes have extra structures in the high binding energy region. A notable example in metals is a satellite peak on the 2p XPS in Ni metal, which appears around 6 eV higher than the threshold.⁵ Feldkamp and Davis⁶ analyzed the Ni 2p XPS spectra by evaluating the overlap determinants between the ground and excited states, using a numerical method on the Hubbard-like model. They clarified the origin of satellite as a combined effect of the core-hole screening and the interaction between electrons, and estimated the strength of the core-hole potential consistent with the binding energy of the satellite intensity and the asymmetry parameter.

In addition to the above features, core-level XPS spectra present several intriguing behaviors in ferromagnetic transition metals Fe, Co, and Ni. On the spin resolved 3s spectra, they show characteristic satellite intensities in the majority spin channel for all Fe, Co, and Ni, while they show almost single peak structures in the minority spin channel. In Fe, the spectra exhibit particularly a large satellite structure only in the majority spin channel. In contrast to the 3s spectra, the 2p spectra do not have a clear satellite peak in Fe, while they show the notable 6-eV satellite in Ni. As regards the peak around the threshold in 2s, 2p, and 3s spectra, its positions noticeably depend on the spin channel in Fe, while such dependence has not been observed in Ni.^{7,8} According to the recent hard x-ray photoemission spectroscopy

(HAXPES) experiment,⁹ such magnetic splitting is estimated about 0.9 eV for the $2p_{3/2}$ core in ferromagnetic Fe. Similar magnetic splittings have also been observed on the $2p_{3/2}$ spectra in several half-metallic ferromagnetic Heusler alloys.¹⁰⁻¹⁴ Such splittings are usually considered to be related with the local spin moment at the photo-excited site. As regards the satellite structure, it has been clearly observed in the 3s XPS in several Fe compounds.⁷ We have clarified the origin of the satellite intensity on the 3s spectra and that the satellite intensity is not a direct reflection of the local spin moment by calculating the XPS spectra on the *ab initio* level.^{15,16}

For the strongly correlated localized electron systems such as the 3d transition metal oxides and the *f*-electron systems, the theoretical analysis of the XPS spectra have been carried out mainly on the basis of atomic, cluster, or impurity Anderson models.¹⁷ Although the impurity Anderson model has been applied to analyze the core-level spectra in some itinerant metallic systems,^{12,18} it is not suitable to analyze the spectra in the highly itinerant metallic systems. Another approach to investigate the core-level spectra is based on the independent one-electron theory exploiting a meanfield approximation. Mahan,¹⁹ and Barth and Grossmann²⁰ have calculated the overall line shapes of the x-ray spectra by evaluating one-electron wave functions under the final state potential, and have reproduced well the experimental emission and absorption spectra in metals within the meanfield theory.

Recently we have presented the XPS spectra based on the *ab initio* band structure calculation.^{15,16} We have calculated the final state potential self-consistently by carrying out the band structure calculation on the system holding a core-hole at a photo-excited site. Not only the core-hole potential but also the relaxation of the core states as well as the screening electron distribution are automatically determined through the calculation. Dis-

tributing electrons on the energy levels thus evaluated, we have constructed various final states. We have evaluated the overlaps between those final states and the ground states by using the one-electron wave functions, and finally obtained the 3s core-level XPS spectra in the ferromagnetic transition metals Fe, Co, and Ni. The element and photo-electron-spin dependence of the spectral line shape have been reproduced in good agreement with experiments within the *ab initio* manner.^{15,16} This method may be regarded as an extension of the Feldkamp-Davis method⁶ to an *ab initio* level. The origin of the spectral shape as a function of the binding energy has been elucidated in terms of the one-electron states screening the core-hole as follows.

In the fully screened state where an up-spin 3s electron is removed, the down-spin 3d states are strongly attracted in the core-hole site, forming quasibound states near the bottom of the 3d band (hereafter majority spin and minority spin are called as up-spin and down-spin, respectively). The final states that the quasibound states are unoccupied contribute to the satellite or shoulder intensities. In the state where a down-spin 3s electron is removed, the up-spin 3d electrons are strongly attracted to the core hole, forming quasibound states near the bottom of the 3d band, but the down-spin 3d electrons are not attracted strongly enough to form quasibound states. Because the up-spin 3d states are almost fully occupied in the ground state, the quasibound states, which appear only in the up-spin 3d states, could not become unoccupied, leading to a single peak structure of the spectra.

In this paper, we apply our method to calculate the 2p core-level XPS spectra in ferromagnetic Fe, Co, and Ni, and elucidate the underlying mechanism. The calculation could not distinguish between the 2p_{3/2} core and the 2p_{1/2} core, because the spin-orbit interaction is not taken into account. We focus on the difference of the spectra among the three ferromagnetic transition metals and on the difference between the 2p and 3s spectra. The main features of the 2p spectra are consistently reproduced in the same manner as those of 3s spectra. We could understand the origin of the spectral shape in the high binding energy region by considering an electron-hole pair excitation from the quasibound states with down-spin to the unoccupied states in the fully screened state. In Ni, the fully screened one-electron states are similar both in the 2p and 3s electron removal states, while they are significantly different in Fe. Such different screening behaviors of the 3d states cause the difference in the spectral shapes between Fe and Ni. It is found that the band filling in the down-spin state plays important roles to give rise to the difference between the Fe 2p and Ni 2p spectra. We also evaluate the magnetic splitting of the threshold energy, exploiting the coherent potential approximation (CPA) within the fully screened potential approximation. This may be observed as the magnetic splitting of the peak position around the threshold in the spin-resolved XPS spectra. We obtain the magnetic splitting of Fe 2p_{3/2} as 0.9 eV in agreement with the recent experiment, and that

of Ni 2p_{3/2} as nearly zero despite the finite local magnetic moment about 0.6 μ_B .

The present paper is organized as follows. In Sec. II, we briefly describe the calculation procedure of the XPS spectra. In Sec. III, we present the 3d band calculated in the presence of core hole and the XPS spectra in comparison with the experiments. The last section is devoted to the concluding remarks.

II. CALCULATION METHOD

A. Calculation of spectral intensity

We briefly summarize the calculation procedure for the core-level photoemission spectra. For details, we refer the readers to Ref.[16]. The many-body wave functions of the ground and final states are assumed to be given as single Slater determinants.

For the ground state, we carry out the full potential linear augmented plane wave (FLAPW) band structure calculation based on the local density approximation (LDA), and obtain the one-electron wave functions ϕ_j 's. We construct the Slater determinant by putting electrons from the lowest energy state up to the Fermi level. For the final states, we carry out the same type of band calculation under the fully screened potential in a periodic array of supercells with one core hole per cell. The core-states are treated as localized states within a muffin-tin sphere, so that we could specify the core-hole site. In reality, only one core-hole should exist in crystal through the XPS event. Therefore, the larger the unit cell size is, the better results would be expected to come out. We use the $3 \times 3 \times 3$ bcc supercell for Fe and fcc supercell for Co and Ni, where the core-hole sites form a bcc super lattice and an fcc super lattice, respectively. In the self-consistent procedure, we keep a hole in a specified core level at a core-hole site, and put an extra electron in each super cell to guarantee the charge neutrality. The local charge neutrality would be satisfied, known as the Friedel sum rule in the impurity problem.²¹ We thus obtain the one-electron wave function ψ_i with energy eigenvalue ϵ_i , which takes account of not only the effect of core-hole potential but also that of electron-electron interactions within the limit of the LDA. The final state $|f(0)\rangle$ with the lowest energy is constructed by putting electrons from the lowest energy state up to the Fermi level at each \mathbf{k} point, as was done in the ground state. The other final states are obtained by creating electron-hole (e-h) pairs from this final state $|f(0)\rangle$. We designate the state having the ℓ e-h pairs on the state $|f(0)\rangle$ as $|f(\ell, m)\rangle$, where the index m distinguishes the different electron configuration. The overlap integral $a_{i,j}^{(\ell,m)}$ between the wave function $\psi_{i(\ell,m)}$ for the i 'th occupied valence state in the final state $|f(\ell, m)\rangle$ and the wave function ϕ_j for the j 'th occupied valence state in the ground state $|g\rangle$ is given by as $a_{i,j}^{(\ell,m)} = \int \psi_{i(\ell,m)}^* \phi_j d\mathbf{r}^3$, where the volume integral is

taken over a super cell.

Neglecting the interaction between the escaping photoelectron and the other electrons in matter, we consider the XPS process that a core-electron is excited to a high energy state with energy ϵ by absorbing an x-ray photon with energy ω . Exploiting Fermi's golden rule, we obtain the expression of the spectral intensity as a function of the binding energy $\omega - \epsilon$ as

$$I_{\sigma}^{\text{XPS}}(\omega - \epsilon) = A \sum_{\ell, m} \left| \begin{matrix} a_{1,1}^{(\ell, m)} & \cdots & a_{1, N_e}^{(\ell, m)} \\ \vdots & a_{i,j}^{(\ell, m)} & \vdots \\ a_{N_e, 1}^{(\ell, m)} & \cdots & a_{N_e, N_e}^{(\ell, m)} \end{matrix} \right|^2 \times \delta(\omega - \epsilon - E_0 + E_g - \Delta E_{(\ell, m)}), \quad (1)$$

where E_0 and E_g represent the total energy of the final state $|f(0)\rangle$ and the ground state $|g\rangle$, A is an energy independent constant including the contribution of overlaps between the wave functions of the core-state in the final and ground states. N_e is the number of valence electrons in the ground state. The overlaps between the valence states and the core states are eliminated because they could be almost orthogonal. $\Delta E_{(\ell, m)}$ is the excitation energy defined by $\Delta E_{(\ell, m)} = E_{(\ell, m)} - E_0 = \sum_{(n, n')} (\epsilon_n - \epsilon_{n'})$, where $E_{(\ell, m)}$ represents the total energy of the final state $|f(\ell, m)\rangle$ and ϵ_n 's are the Kohn-Sham eigenvalues. The energy difference $\epsilon_n - \epsilon_{n'}$ stands for the energy of an e-h pair of an electron at level n and a hole at level n' and the summation are taken over all e-h pairs in the final state $|f(\ell, m)\rangle$. Although the Kohn-Sham eigenvalues may not be proper quasi particle energies, they practically give a good approximation to quasiparticle energies, except for the fundamental energy gap.^{22,23} In the following calculation, we replace the δ function by the Lorentzian function with the full width at half maximum (FWHM) $2\Gamma = 1$ eV in order to take into account the lifetime broadening of the core level. $E_0 - E_g$ is treated as an adjustable parameter so that the threshold of XPS spectra coincides with the experiments. In order to suppress the error caused by the fictitious periodicity of the core-hole site, we pick up only the Γ point as the sample states for calculating XPS spectra. For Ni, we pick up the X point $(\frac{1}{2}, 0, 0)$ as a sample point in addition to the Γ point, because the $3d$ band states at the Γ point are fully occupied by both up- and down-spin electrons on the system of the $3 \times 3 \times 3$ fcc super-cell. We take account of the final states including 0, 1, 2, and 3 electron-hole pairs on the final state $|f(0)\rangle$ and restrict the final states $|f(\ell, m)\rangle$ so that the excitation energy $E_{(\ell, m)} - E_0$ is less than 10 eV. We need to calculate the more than 10^8 determinants of the matrices of the size of about 150×150 for Fe even after the above simplification.

Before closing this subsection, we briefly mention the limitations in this calculation. First, we assume that the $2p$ core hole is spherically distributed with neglecting the dependence on the magnetic quantum number of the core hole. Second, we take no account of the spin-orbit interaction (SOI) in the band structure cal-

culation. Third, due to the finiteness of the cell size, the final state $|f(0)\rangle$ (no e-h pair) has a finite overlap with the ground state $|g\rangle$, resulting in a finite intensity at the threshold. In principle, such overlap should converge to zero with $N_e \rightarrow \infty$, according to the Anderson orthogonality theorem;¹ energy levels become continuous near the Fermi level and thereby infinite numbers of e-h pairs could be created with infinitesimal excitation energies, leading to the so-called Fermi edge singularity in the XPS spectra. The finite contribution obtained above arises from the discreteness of energy levels and could be interpreted as the integrated intensity of singular spectra near the threshold, in consistent with the model calculations for other systems.^{6,24}

B. Binding energy difference at the threshold

The threshold energies $\omega_{\uparrow}^{\text{th}}$ for the up-spin core-electron removal excitation and $\omega_{\downarrow}^{\text{th}}$ for the down-spin one are generally different in the ferromagnetic systems. It could be naively considered that the difference $\Delta\omega^{\text{th}} = \omega_{\uparrow}^{\text{th}} - \omega_{\downarrow}^{\text{th}}$ is linked to the energy difference between the up- and down-spin core levels in the ground state and is a good indicator for the local spin moment. However, because of the considerable core-hole screening in metals, the final state effects should be taken into consideration. Within the fully screened potential approximation, we may obtain a better estimate of $\Delta\omega^{\text{th}}$ without using supercell but by using the CPA in the low concentration limit, as was done in the calculation of the core-level chemical shift in metallic random alloys.^{25,26} Because the core-hole screening is almost completed within the core-hole site for metals, the CPA, which is a one-site approximation, may not cause large error.

The threshold energy may be written as

$$\omega_{\uparrow(\downarrow)}^{\text{th}} = E_{\uparrow(\downarrow)} - \epsilon_F - E_g, \quad (2)$$

where E_g represents the total energy of the ground state, $E_{\uparrow(\downarrow)}$ does that of the fully screened state with an up(down)-spin core hole and $N_e + 1$ band electrons, and ϵ_F is the Fermi energy in the fully screened state. Therefore, the difference may be given by

$$\Delta\omega^{\text{th}} = \omega_{\uparrow}^{\text{th}} - \omega_{\downarrow}^{\text{th}} = (E_{\uparrow} - E_g) - (E_{\downarrow} - E_g). \quad (3)$$

The energy difference $E_{\uparrow(\downarrow)} - E_g$ corresponds to the energy of putting one core-ionized impurity at a normal site. This might be given as the generalized thermodynamic chemical potential,

$$E_{\uparrow(\downarrow)} - E_g = \left. \frac{\partial \bar{E}_{\uparrow(\downarrow)}(\rho)}{\partial \rho} \right|_{\rho \rightarrow 0}, \quad (4)$$

where $\bar{E}_{\uparrow(\downarrow)}$ represents the total energy per unit cell for the random alloy system which consist of core-ionized and normal atoms and ρ the density of the cell including a

core-hole site. Hence, the difference $\Delta\omega^{\text{th}}$ may be written as

$$\Delta\omega^{\text{th}} = \frac{d}{d\rho} (\overline{E}_{\uparrow}(\rho) - \overline{E}_{\downarrow}(\rho)) \Big|_{\rho \rightarrow 0}. \quad (5)$$

We evaluate these values with the help of the KKR Green's function band structure calculation combined with CPA.^{27,28} We carry out the calculation at the concentration ranged from $\rho = 0$ to 0.05. $\Delta\omega^{\text{th}}$ is calculated by an extrapolation to zero concentration ρ .

III. RESULTS AND DISCUSSIONS

A. Ground and fully screened states

1. *d*-DOS

We carry out the band structure calculation based on the LDA. For the $2p$ electron removal, we make the FLAPW super cell calculation. The magnetic moments in the ground states are obtained 2.1, 1.6, and $0.6 \mu_B$ inside a muffin-tin sphere ($r_m = 2.0$ Bohr) for Fe, Co, and Ni, respectively. The obtained electronic structures in the ground states are consistent with the past band structure calculations.²⁹ We have also checked the accuracy of the calculation by carrying out the KKR band structure calculation combined with the CPA.^{27,28} We treat the system as a random alloy system consisting of the normal and core-ionized atoms, and take the limit of zero concentration of the core-ionized atom. The FLAPW supercell calculation and the KKR-CPA calculation give essentially the same results.

The one-electron states in the fully screened state are modified from those in the ground state by the core-hole potential. Such changes in one-electron states may be explained through the change in the *d*-symmetric density state (*d*-DOS) at the core-hole site. Figure 1 shows the *d*-DOS at the core-hole site. The *d*-DOS's at the core-hole site in the fully screened states are greatly modified from those in the ground state. The *d*-DOS at sites with no core hole, which are not shown here, are almost unchanged from those in the ground state. This indicates that the core-hole potential is almost completely screened inside the core-hole site, being consistent with the small screening length \sim Bohr radius for metals. The change of the *d*-DOS's by the core-hole potential depends largely on whether the up- or down-spin electron is removed from the $2p^6$ core state. We refer to the hole created in the $2p$ states by removing an up(down)-spin electron as the up(down)-spin hole.

In the fully screened state with an up-spin $2p$ hole, the weight of the down-spin *d*-DOS moves toward the higher binding energy region if compared with the up-spin *d*-DOS. This is due to the repulsive (attractive) exchange interaction working between the up-spin hole and the up(down)-spin $3d$ electrons, in addition to the attractive interaction between the core hole and $3d$ electrons.

In Ni, the weight of the *d*-DOS of the down-spin state concentrate near the bottom of the $3d$ band, indicative of the quasibound states. The weight of the up-spin states also shifts toward to the higher binding energy region. These behaviors are very similar to those for the $3s$ electron removal. In Co, the weight of the *d*-DOS's of the down-spin $3d$ states shifts toward the higher binding energy region. Opposite to the case for Ni, that weight of the up-spin $3d$ states shifts toward the Fermi level. The behaviors are similar to those for the $3s$ electron removal but with rather moderate shape. In Fe, the weight of the *d*-DOS's of the down-spin $3d$ state moves toward the higher binding energy region, but not as much as for Ni. The weight of the up-spin $3d$ states is almost unchanged. The behavior in Fe contrasts to that for the $3s$ electron removal, where the weight of the down-spin *d*-DOS highly concentrates near the bottom of the $3d$ band and that for the up-spin *d*-DOS significantly shift toward the Fermi level.

In the fully screened state with a down-spin $2p$ hole, the weight of the up-spin *d*-DOS's tends to move toward the higher binding energy region probably due to the exchange interaction between the core hole and the $3d$ electrons. In Fe, the weight of the up *d*-DOS is moderately shifted toward the higher binding energy region compared to the case of the down-spin $3s$ electron removal. The weight of the down-spin *d*-DOS also slightly moves toward the higher binding energy region. In Ni, the shift of the up-spin *d*-DOS is large, indicative of the quasibound states. The weight of the down-spin *d*-DOS also concentrates near the bottom of the $3d$ band. This behavior in Ni is very similar to that for the down-spin $3s$ electron removal. The behavior of the *d*-DOS's in Co is intermediate between Fe and Ni. To sum up, the $3d$ states in Fe for the $2p$ electron removal are quite different from those for the $3s$ electron removal, while those in Ni are quite similar in both removal states.

2. Screening electron number

The change of the *d*-DOS's is related to the screening electron number at the core-hole site. Table I shows the screening electron numbers $\Delta n_{d\uparrow}$, $\Delta n_{d\downarrow}$, and $\Delta n_{d\uparrow} + \Delta n_{d\downarrow}$. Here $\Delta n_{d\uparrow(\downarrow)}$ is given by $\Delta n_{d\uparrow(\downarrow)} = n_{d\uparrow(\downarrow)}^{\text{sc}} - n_{d\uparrow(\downarrow)}^{\text{gr}}$, where $n_{d\uparrow(\downarrow)}^{\text{sc}}$ is the up(down)-spin electron number inside the muffin-tin sphere in the *d*-symmetric states in the core-hole site in the fully screened state, and $n_{d\uparrow(\downarrow)}^{\text{gr}}$ is the corresponding quantity in the ground state. Total screening electron numbers $\Delta n_{d\uparrow} + \Delta n_{d\downarrow}$ inside the muffin-tin sphere is found to be roughly unity. On the sites with no core hole, the electron numbers are almost unchanged from that in the ground state, indicating that the core-hole screening is almost completed inside the core-hole site.

First we discuss the case that an up-spin $2p$ electron is removed. In the fully screened state of Co, the core hole attracts so strongly the down-spin $3d$ electrons that

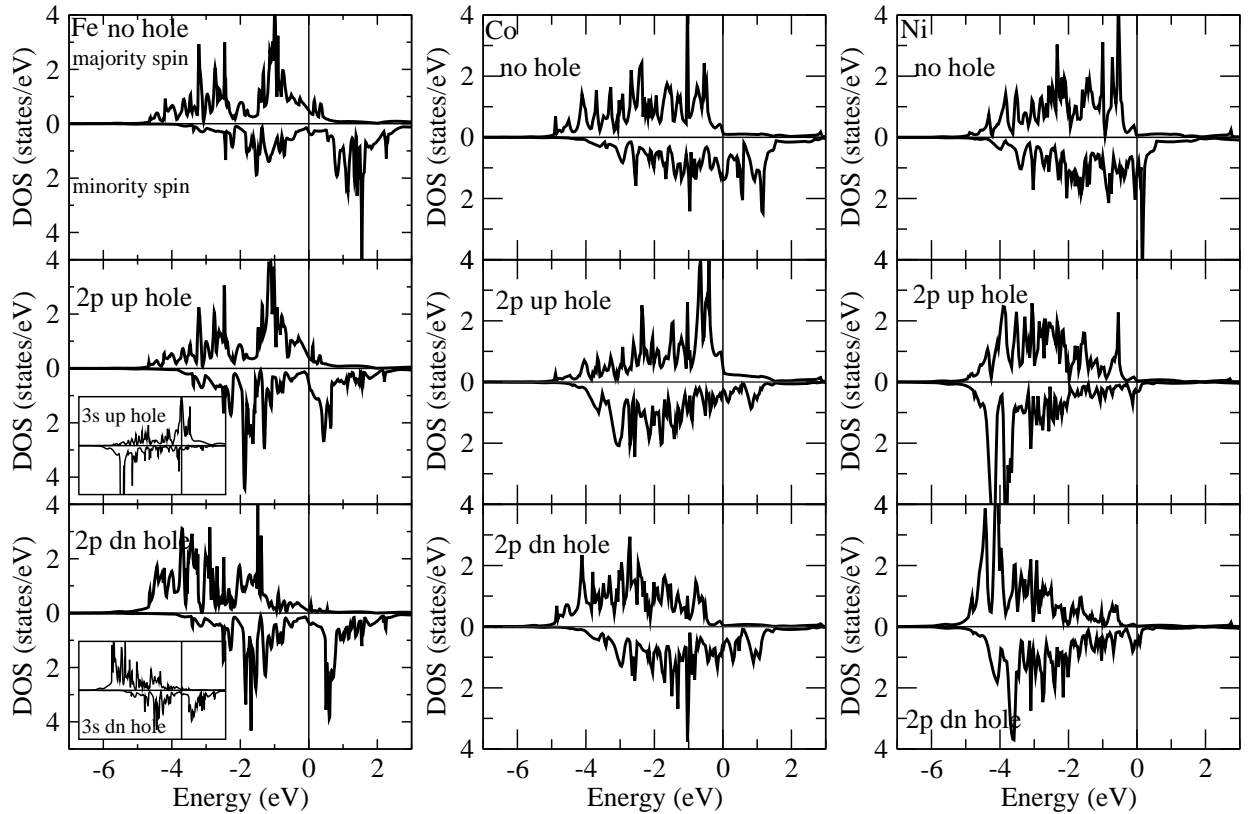


Figure 1: Density of state projected onto the state with d symmetry inside the muffin-tin sphere (d -DOS) at the core-hole site in Fe, Co, and Ni. Top panels show the d -DOS's in the ground states. Middle (bottom) panels show those in the fully screened states with an up (down)-spin $2p$ core-hole. The d -DOS's in the fully screened states with a $3s$ hole are also shown as inset. The energy of the Fermi level is zero.

they overscreen the core hole, and, as a countereffect, a few up-spin $3d$ electrons at the core-hole site are pushed away from the muffin-tin sphere due to the Coulomb repulsion with the excess down-spin electrons. In the fully screened state of Ni, although the strong attraction by the core hole is expected to work on the down-spin electrons, the screening down-spin electron number is less than unity, because the d states at the core-hole site are already almost filled in the ground state. The up-spin $3d$ electrons participate a little to screen the core-hole. Note that those screening electron numbers are similar to those for the up-spin $3s$ electron removal state both in Co and Ni. In Fe, the screening of the core hole is almost completed by the down-spin $3d$ electrons without overscreening. This is quite different from the fully screened state for the up-spin $3s$ electron removal, where the down-spin $3d$ electrons extremely overscreen the core hole, and that overscreening is compensated by pushing away the up-spin $3d$ electrons from the core hole site. Now we discuss the case that a down-spin $2p$ electron is removed. In the fully screened states of Ni, although the up-spin $3d$ electrons are to be strongly attracted by the core hole, the screening electron number is not large, because the up-spin $3d$ state is almost filled in the ground state. Therefore, the down-spin $3d$ electrons contribute

Table I: Screening electron number with the d symmetry inside the muffin-tin sphere at the $2p$ core hole site. The radii of the muffin-tin spheres are 2.0 Bohr.

	$2p$ hole	$\Delta n_{d\uparrow}$	$\Delta n_{d\downarrow}$	$\Delta n_{d\uparrow} + \Delta n_{d\downarrow}$
Fe	Up	0.19	1.01	1.20
	Down	0.47	0.67	1.14
Co	Up	-0.14	1.35	1.21
	Down	0.22	0.86	1.08
Ni	Up	0.18	0.89	1.07
	Down	0.27	0.79	1.06

in large amount, leading that the total screening numbers become nearly unity. In the fully screened states of Fe and Co, although the up-spin $3d$ electrons are more attracted by the core hole than the down-spin electrons, the screening electron number of the up-spin electron is smaller than the down-spin electrons for a similar reason to Ni.

3. Difference between the $2p$ core electron removal and the $3s$ -core electron removal

Now we focus on the difference in the screening behavior between with the $2p$ core hole and the $3s$ core hole. For both cases, the down(up)-spin $3d$ electrons are, generally speaking, attracted to the core hole more strongly than the up(down)-spin $3d$ electrons in the fully screened state both with an up(down)-spin $2p$ or $3s$ core hole, because the exchange interaction is working between the core hole and the $3d$ electrons. In addition to this tendency, the screening in Fe seems moderate in the fully screened state with a $2p$ core hole, compared to the presence of the overscreening with a $3s$ core hole. On the other hand, in Ni, the screening with a $2p$ core hole is comparably larger than that with a $3s$ core hole. How does such a different screening behavior occur in Fe and Ni? The exchange interaction J_{2p-3d} between the $2p$ and $3d$ electrons, and J_{3s-3d} between the $3s$ and $3d$ electron may be estimated by the atomic Hartree-Fock calculation, which are $J_{2p-3d} \sim 1$ eV and $J_{3s-3d} \sim 2$ eV, for all the neutral Fe, Co, and Ni atoms, respectively. The small $2p$ - $3d$ exchange interaction in Fe could not solve the above question.

To eliminate the effect of the $2p$ - $3d$ ($3s$ - $3d$) exchange interaction, we carry out the band calculation under the condition that a half up-spin and a half down-spin electron is removed from the $2p$ ($3s$) core states. Figure 2 shows the d -DOS's at the core hole site in the fully screened state. The d -DOS's for the state with a $2p$ core hole are similar to those with a $3s$ core hole. Note that the atomic Hartree-Fock calculation gives quite different values of the Slater integrals F^0 's for $2p$ - $3d$ and $3s$ - $3d$ interactions, that is, $F^0(2p, 3d) - F^0(3s, 3d) \sim 7$ eV, which in fact contradicts the results shown in Fig. 2. In Ni, the d -DOS's concentrate near the bottom of the up- and down-spin $3d$ band, forming quasibound states. In Fe, the situation is quite different; the weights of the d -DOS shift only moderately toward the higher binding energy region, almost keeping the structures of the ground state. In Co, the behavior of the d -DOS is intermediate between Fe and Ni. This difference in Fe, Co, and Ni may be related to the different electron occupation in the band in the ground state. In Ni, because the $3d$ band is almost fully occupied, it is hard to make enough room for accommodating the screening electron at the core hole site by mixing the one-electron states within the $3d$ band states. Therefore, the mixing beyond the $3d$ band states has to take place to complete core hole screening inside the core hole site. These processes might help to form quasibound states. In Fe, because the $3d$ band in the ground state has enough room to accommodate excess screening electron, the mixing of the one-electron states within the $3d$ band states might be sufficient in order to complete core hole screening, resulting in only the slight shift of the weight of the d -DOS's. When the $2p$ - $3d$ ($3s$ - $3d$) exchange potential is turned on, the screened states get modified further. In Ni, both the $2p$ - $3d$ and $3s$ - $3d$ ex-

change potentials simply shift the quasibound states to the higher or lower binding energy regions. In Fe, the $3s$ - $3d$ exchange potential considerably modify the $3d$ state by pulling down the down-spin $3d$ states at around 0.5 eV above the Fermi level (the top panel in Fig. 2) under the Fermi level, and by making the quasibound states formed near the bottom of the down-spin $3d$ band. The $2p$ - $3d$ exchange potential, on the other hand, hardly affects the $3d$ band states, that is, the down-spin $3d$ states at around 0.5 eV still stay above the Fermi level probably due to the smallness of the $2p$ - $3d$ exchange potential.

B. Photoemission Spectra

Using the one-electron wave functions in the ground state and fully screened states, the XPS intensities are calculated as a function of the binding energy from eq. (1). Figures 3-5 show the calculated spectra for bcc Fe, fcc Co, and fcc Ni, in comparison with the experimental $2p_{3/2}$ spectra. Although the edge singularity is not reproduced, the overlaps $\langle f(0) | g \rangle$ and $\langle f(1, m) | g \rangle$'s appear to give the reasonable intensities around threshold. The total spectral curves, which depend on the elements, reproduce well the overall structures observed in the experiments. Note that the final states $|f(1, m)\rangle$'s holding a down-spin e-h pair mainly contribute to the intensity. The final state $|f(1, m)\rangle$'s created by putting an up e-h pair on the final state $|f(0)\rangle$ hardly contribute to the intensity, because the up-spin $3d$ band states are almost filled in the ground state, and thereby the overlap determinant become quite small.

The Fe spectra show a single-peak structure with a weak shoulder intensity for both the up- and down-spin $2p$ electron removals, contrasting with the strong satellite intensity for the up-spin $3s$ electron removal. Because the one-electron wave functions in the fully screened state are not so strongly modified from those in the ground state, the overlap $\langle f(0) | g \rangle$ is almost unity. Consequently, the other overlaps $\langle f(\ell, m) | g \rangle$'s are almost zero, because the one-electron wave functions for the unoccupied states in the final state $|f(0)\rangle$ are nearly orthogonal to those for occupied states in the ground state $|g\rangle$. Note that the observed 0.9 eV splitting of the peak position around the Fe $2p_{3/2}$ threshold is not reproduced by the e-h excitations on the final state $|f(0)\rangle$. We expect that the splitting originates from the different threshold energy for the up- and down-spin $2p$ electron removals.

In Co, the intensities at the higher binding energy region are larger than the Fe $2p$ spectra, forming a rather strong shoulderlike structure for the up-spin $2p$ electron removal. Because the one-electron wave functions for the down-spin $3d$ band states in the fully screened state are noticeably modified from those in the ground state, the one-electron wave functions of the unoccupied levels in the final state $|f(0)\rangle$ have some amplitudes of those of the occupied levels in the ground state. The overlaps $\langle f(\ell, m) | g \rangle$'s accordingly become finite, giving rise to the

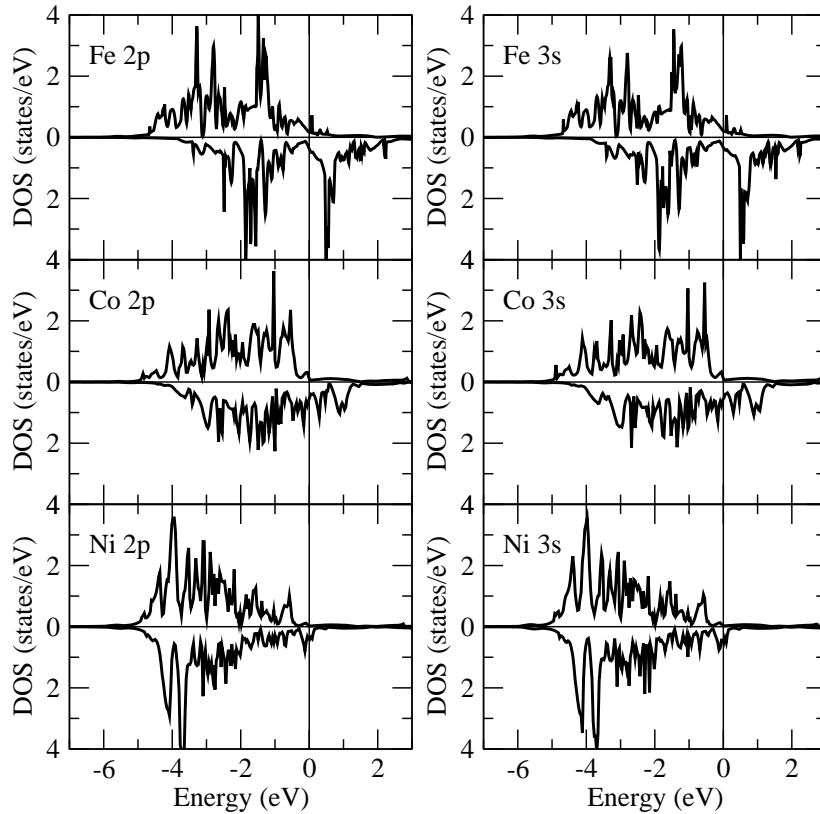


Figure 2: d -DOS's when removing a half up- and a half down-spin electron from the $2p$ and $3s$ core. The energy of the Fermi level is zero.

shoulder. For the down-spin $2p$ electron removal, the spectra show a single-peak structure, because the down-spin $3d$ states are not strongly modified by the down-spin $2p$ hole.

The Ni spectra exhibit satellite structure for the up-spin $2p$ electron removal. The e-h pair excitations that an electron on the quasibound state is excited to the unoccupied states give rise to the satellite intensity. The satellite peak position is around 4 eV, which is 2 eV smaller than the so-called 6-eV satellite observed in experiment. This discrepancy might be caused by the LDA or the fully screened potential approximation. Because both the up- and down-spin $3d$ states are fully occupied in the fully screened state, the $3d$ - $3d$ Coulomb interaction may not be relevant to this discrepancy within the fully screened potential approximation. Braicovich and van der Laan³² estimated the screening time constant $\tau_s = 1.5$ fs in Ni, which is definitely longer than the values 0.18 fs in Fe and 0.43 fs in Co. Because the constant τ_s is comparable to the core hole lifetime $\tau_c \sim 1$ fs, the use of the fully screened potential may not be appropriate to describe the satellite intensities in Ni. The spectra for the down-spin electron removal also show relatively large shoulder intensities, which would come from the excitations in the down-spin $3d$ states, because the unoccupied levels are available in the down-spin $3d$ states in the fully screened $3d$ states.

C. Energy difference of the threshold

In order to estimate the magnetic splitting of the threshold energy, we calculate the energy difference of the threshold in the up- and down-spin core-electron removals by using the KKR-CPA method, as discussed in Sec. II B. Figures 6 and 7 show the energy difference of the threshold $\Delta\omega^{\text{th}}$ defined by Eq. (5) and the energy difference of the core levels $\Delta\epsilon^c = \epsilon_{\downarrow}^c - \epsilon_{\uparrow}^c$ in the ground states. While $\Delta\epsilon^c$'s are nearly proportional to the local spin moment, $\Delta\omega^{\text{th}}$'s decrease more rapidly than the change of the local moments with moving from Fe to Ni. In Fe, we get the local moment about $2.2 \mu_B$ and $\Delta\omega^{\text{th}}$'s about 1.2, 0.9, and 1.5 eV for the $2s$, $2p$, and $3s$ excitations, respectively. In Ni, on the other hand, $\Delta\omega^{\text{th}}$'s are almost zero, despite the definite local spin moment about $0.6 \mu_B$. These values seem to be consistent with the experimental observations; the splitting is estimated as $\gtrsim 1$ eV in the Fe $3s$ spin resolved spectra,⁷⁻⁹ and 0.9 eV in the Fe $2p_{3/2}$ HAXPES spectra.⁹ On the other hand, such splittings have not been observed in the Ni $2p$ and $3s$ spectra.

It is obvious that the core hole screening plays crucial roles in determining the magnitude of the splitting of the threshold energy. The fact that the magnetic splitting in Ni is smaller than that in Fe may be understood as follows. All the $3d$ states in the fully screened state in

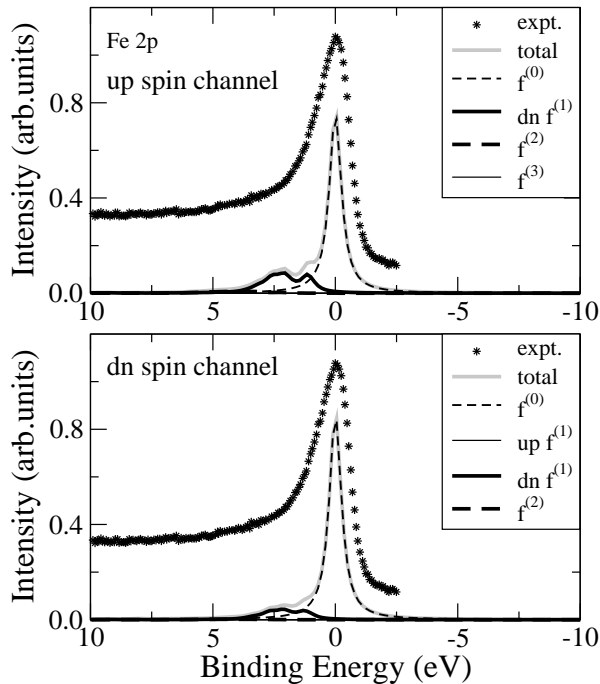


Figure 3: Fe 2p XPS spectra. Gray thick curve represents the total intensity. The curves denoted $f^{(0)}$, up $f^{(1)}$, dn $f^{(1)}$, $f^{(2)}$, and $f^{(3)}$ are the contribution from the final states including zero, one up-spin e-h pair, one down-spin e-h pair, two e-h pairs, and three e-h pairs on the final state $|f(0)\rangle$, respectively. Experimental data are taken from Ref. 7, which are not spin resolved.

Ni are pulled down below the Fermi level forming the quasibound states resulting in a suppression of the local spin moment at the core hole site solely by the Coulomb interaction between the core hole and the 3d electrons (Fig. 2). The exchange potential could not give rise to a large difference in the screening electron distribution between for the up-spin and down-spin electron removals. The 3d states in Fe, on the other hand, are strongly affected by the exchange potential particularly for the 3s electron removal, with the considerable change of the d -DOS's and with the screening electron numbers. Even for the 2p electron removal, the screening electron numbers depend considerably on the spin channel. Thus we may guess that the weak effect of the exchange potential on the 3d states in Ni may be the origin of the magnetic splitting of the threshold energy. Note that the zero magnetic splitting does not necessarily mean that the XPS spectra for the up-spin channel are the same as those for the down-spin channel.

IV. CONCLUDING REMARKS

We have applied an *ab initio* method to calculate the 2p core-level XPS spectra as a function of binding energy in ferromagnetic metals Fe, Co, and Ni. The calculated

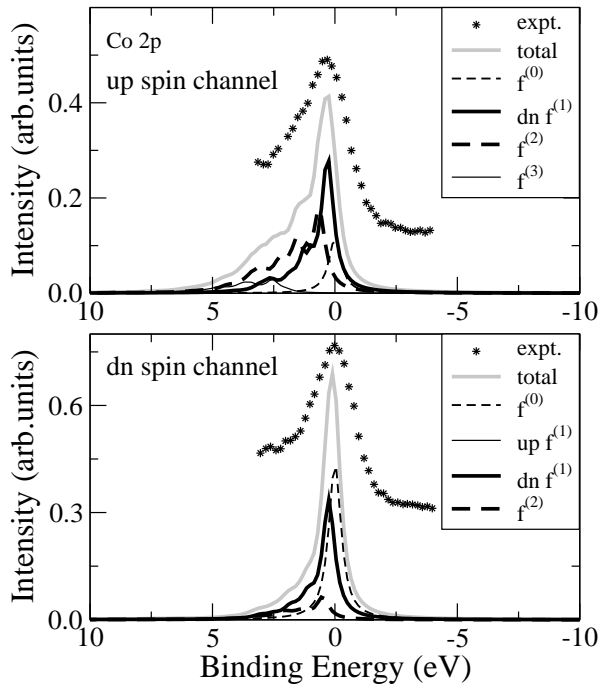


Figure 4: Co 2p XPS spectra. Gray thick curve represents the total intensity. The curves denoted $f^{(0)}$, up $f^{(1)}$, dn $f^{(1)}$, $f^{(2)}$, and $f^{(3)}$ are the contribution from the final states including zero, one up-spin e-h pair, one down-spin e-h pair, two e-h pairs, and three e-h pairs on the final state $|f(0)\rangle$, respectively. Spin-resolved experimental data are taken from Ref. 30.

spectra have been compared to the spin-resolved $2p_{3/2}$ spectra, where the up- and down-spin electron removal excitations are considered separately. Because the SOI is not included in the calculation, we could not distinguish $2p_{3/2}$ and $2p_{1/2}$. The dependence of the spectral shapes on the element, the excited core, and the spin of the core hole left behind are well reproduced by the calculation. The Fe 2p spectra show almost a single-peak structure for the up-spin and down-spin electron removals. In contrast, the spectral intensities for Ni are distributed in a wide range of binding energy with the notable satellite structure for the up-spin electron removal and the shoulder-like structure for the down-spin electron removal. The spectra for Co exhibit intermediate features between those for Fe and Ni; the spectra are widely distributed around the higher binding energy region with noticeable shoulder structure for the up-spin electron removal, while the spectra exhibit almost a single-peak structure for the down-spin electron removal. The satellite intensities in Ni 2p spectra are interpreted as coming from the final state that an electron on the quasibound state is excited to the unoccupied one-electron states on $|f(0)\rangle$. Such satellite or shoulder structures exist in all elements Fe, Co, and Ni for the up-spin 3s electron removal.¹⁶ We have discussed the difference between the 2p and 3s spectra as well as the difference between Fe and Ni spectra in connection with the one-electron

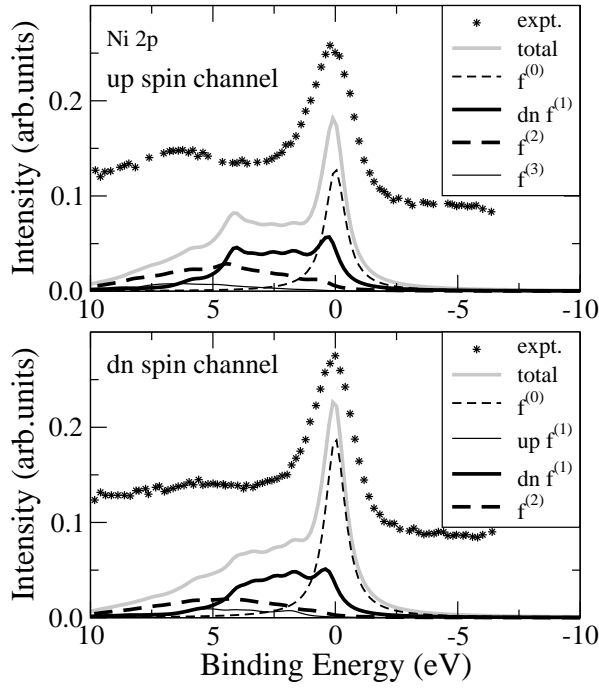


Figure 5: Ni 2p XPS spectra. Gray thick curve represents the total intensity. The curves denoted $f^{(0)}$, up $f^{(1)}$, dn $f^{(1)}$, $f^{(2)}$, and $f^{(3)}$ are the contribution from the final states including zero, one up-spin e-h pair, one down-spin e-h pair, two e-h pairs, and three e-h pairs on the final state $|f(0)\rangle$, respectively. Spin-resolved experimental data are taken from Ref. 31.

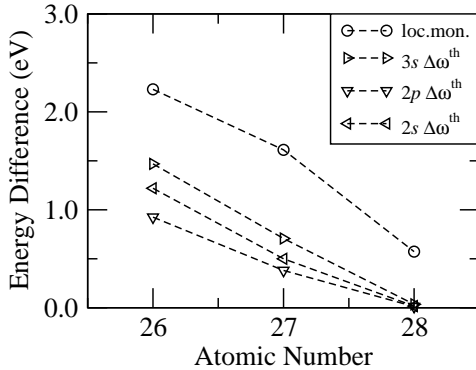


Figure 6: Difference of the threshold energy between the states that an up-spin core-electron is removed and that a down-spin core-electron is removed. Left, down, and right triangles represent $\Delta\omega^{\text{th}}$ for the 2s, 2p, and 3s core-ionized states. Circle represents the local spin moment at the core hole site in μ_B . Dashed lines are for a guide to eyes.

states screening the core hole. We have explained the origin of these differences by a combined effect of the different magnitude of the $2p$ - $3d$ and $3s$ - $3d$ exchange potentials and the different occupation numbers in the $3d$ states in Fe and Ni.

Although the calculation reproduce consistently the spectra shape depending on the elements, the excited

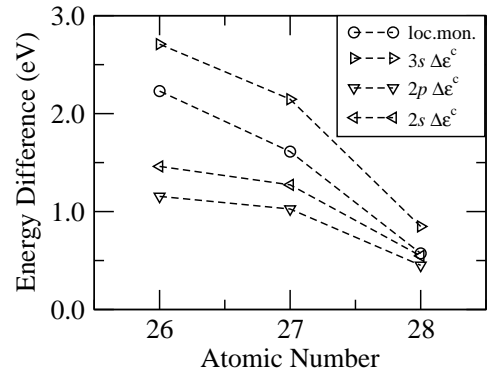


Figure 7: Difference of the up-spin and the down-spin core-level energies. Left, down, and right triangles represent $\Delta\epsilon^c$ for 2s, 2p, and 3s core-ionized states. Circle represents the local spin moment at the core hole site in μ_B . Dashed lines are for a guide to eyes.

core, and the spin of the core hole left behind, there is a clear discrepancy on the satellite position in Ni; 6 eV satellite in Ni that the calculation gives the satellite is given at merely 4 eV higher than the threshold. One reason for this discrepancy may be that the fully screened potential approximation is not appropriate due to the insufficient time of screening core hole in Ni in comparison with the core hole lifetime. Another reason might be caused by the approximate nature of LDA. To clarify this issue, we need further studies.

In connection with the magnetic splittings of the threshold energy, we have directly evaluated these values within the fully screened potential approximation by using the KKR-CPA method. Olovsson *et al.*^{25,26} have discussed the core-level chemical shifts in several metallic alloys using the same method, and pointed out that the fully screened potential approximation gives good correspondence to the experiments. The core-level energy depends on its spin, which difference is roughly proportional to the local spin moment. We have found that the magnetic splitting of the threshold energy decreases more rapidly than the local spin moment with moving from Fe to Ni; it is almost zero for Ni for the 2s, 2p, and 3s electron removals, in spite of a finite local moment $0.6 \mu_B$. The splitting may be directly measured by the shift of the peak around the threshold in the spin resolved 2s or 3s spectra. Actually, in the recent experiment of the $2p_{3/2}$ HAXPES spectra,⁹ such a splitting is measured as 0.9 eV. Our calculation also suggests that the splitting would hardly be observed in Ni. To be more precise, it may be better to take account of the SOI and to increase the super-cell size.

We have considered only the one-electron states on the Γ point in the first Brillouin zone onto which electrons are distributed in the calculation of the XPS spectra. This may not cause large errors except the intensity near the threshold, because the first Brillouin zone is reduced to a smaller size in a system of larger supercells. With increasing the states onto which electrons are distributed,

we expect that the overlap between the lowest energy state in the presence of core hole and the ground states would be reduced, and that the contributions from e-h pair creation would increase near the threshold, leading to an asymmetric peak near the threshold as a function of binding energy. Such behavior has been demonstrated in numerical calculations on finite-size systems.^{6,24} On the other hand, the structures in the high binding energy region are expected to be only a little influenced by such a refined treatment. In any case, to be more quantitative, we need to increase the size of supercells in the calculation.

Another *ab initio* approach has been tried by using multiple scattering theory.³³ Since the experimental data have been accumulated for XPS spectra and the x-ray

absorption spectra near the L edge, the extension of the present method to calculate the absorption spectra is left in future study.

Acknowledgments

We used the FLAPW code developed by Noriaki Hamada, and the KKR-CPA code by Hisazumi Akai. This work was partially supported by a Grant-in-Aid for Scientific Research in Priority Areas (No.22540325) of The Ministry of Education, Culture, Sports, Science, and Technology, Japan.

-
- ¹ P. W. Anderson, Phys. Rev. Lett. **18**, 1049 (1967).
 - ² G. D. Mahan, Phys. Rev. **163**, 612 (1967).
 - ³ P. Nozières and C. T. de Dominicis, Phys. Rev. **178**, 1097 (1969).
 - ⁴ S. Doniach and M. Sunjic, J. Phys. C **3**, 285 (1970).
 - ⁵ S. Hufner and G. W. Wetheim, Phys. Lett. **51A**, 301 (1975).
 - ⁶ L. A. Feldkamp and L. C. Davis, Phys. Rev. B **22**, 3644 (1980).
 - ⁷ J. F. van Acker, Z. M. Stadnik, J. C. Fuggle, H. J. W. M. Hoekstra, K. H. J. Buschow, and G. Stroink, Phys. Rev. B **37**, 6827 (1988).
 - ⁸ D. G. Van Campen and L. E. Klebanoff, Phys. Rev. B **49**, 2040 (1994).
 - ⁹ S. Imada, unpublished (2011).
 - ¹⁰ S. Plogmann, T. Schlathölter, J. Braun, M. Neumann, Y. M. Yarmoshenko, M. V. Yablonskikh, E. I. Shreder, E. Z. Kurmaev, A. Wrona, and A. Ślebarski, Phys. Rev. B **60**, 6428 (1999).
 - ¹¹ A. Ślebarski, M. Nuemann, and B. Schneider, J. Phys. : Condens. Matter **13**, 5515 (2001).
 - ¹² A. K. Shukla, P. Krüger, R. S. Dhaka, D. I. Sayago, K. Horn, and S. R. Barman, Phys. Rev. B **75**, 235419 (2007).
 - ¹³ Y. T. Cui, A. Kimura, K. Miyamoto, M. Taniguchi, T. Xie, S. Qiao, K. Shimada, H. Namatame, E. Ikenaga, K. Kobayashi, et al., Phys. Rev. B **78**, 205113 (2008).
 - ¹⁴ A. X. Gray, J. Karel, J. Minár, C. Bordel, H. Ebert, J. Braun, S. Ueda, Y. Yamashita, L. Ouyang, D. J. Smith, et al., Phys. Rev. B **83**, 195112 (2011).
 - ¹⁵ M. Takahashi, J. Igarashi, and N. Hamada, Phys. Rev. B **78**, 155108 (2008).
 - ¹⁶ M. Takahashi and J.-i. Igarashi, Phys. Rev. B **81**, 035118 (2010).
 - ¹⁷ F. de Groot and A. Kotani, *Core Level Spectroscopy of Solids* (CRC Press, Boca Raton, 2008).
 - ¹⁸ A. Tanaka, T. Jo, and G. A. Sawatzky, J. Phys. Soc. Jpn. **61**, 2636 (1992).
 - ¹⁹ G. D. Mahan, Phys. Rev. B **21**, 1421 (1980).
 - ²⁰ U. von Barth and G. Grossmann, Solid State Commun. **32**, 645 (1979).
 - ²¹ J. Friedel, Nuovo Cim. Suppl. **2**, 287 (1958).
 - ²² M. S. Hybertsen and S. G. Louie, Phys. Rev. B **34**, 5390 (1986).
 - ²³ N. Hamada, M. Hwang, and A. J. Freeman, Phys. Rev. B **41**, 3620 (1990).
 - ²⁴ A. Kotani and Y. Toyozawa, J. Phys. Soc. Jpn. **37**, 912 (1974).
 - ²⁵ I. A. Abrikosov, W. Olovsson, and B. Johansson, Phys. Rev. Lett. **87**, 176403 (2001).
 - ²⁶ W. Olovsson, C. Göransson, L. V. Pourovskii, B. Johansson, and I. A. Abrikosov, Phys. Rev. B **72**, 064203 (2005).
 - ²⁷ H. Akai, J. Phys. Soc. Jpn. **51**, 468 (1982).
 - ²⁸ H. Akai, Phys. Rev. Lett. **81**, 3002 (1998).
 - ²⁹ V. L. Moruzzi, J. F. Janak, and A. R. Williams, *Calculated Electronic Properties of Metals* (Pergamon, New York, 1978).
 - ³⁰ L. E. Klebanoff, D. G. Van Campen, and R. J. Pouliot, Phys. Rev. B **49**, 2047 (1994).
 - ³¹ A. K. See and L. E. Klebanoff, Phys. Rev. B **51**, 11002 (1995).
 - ³² L. Braicovich and G. van der Laan, Phys. Rev. B **78**, 174421 (2008).
 - ³³ P. Kruger and C. R. Natoli, Phys. Rev. B **70**, 245120 (2004).